The effects of Cuprizone on murine subventricular zone-derived neural stem cells and progenitor cells grown as neurospheres

Yamila Azul Molinari
Universidad de Buenos Aires Facultad de Farmacia y Bioquimica
Agustin Jesus Byrne
Universidad de Buenos Aires Facultad de Farmacia y Bioquimica
Maria Julia Perez
Universidad de Buenos Aires Facultad de Farmacia y Bioquimica
Lucas Silvestroff
Universidad de Buenos Aires Facultad de Farmacia y Bioquimica
Paula Gabriela Franco (pgfranco@ffyb.uba.ar)
Universidad de Buenos Aires Facultad de Farmacia y Bioquimica https://orcid.org/0000-0002-0551-791X

Research Article

Keywords: NEUROSPHERES, OLIGODENDROGENESIS, TOXICITY, DIFFERENTIATION, PROLIFERATION, MIGRATION

Posted Date: May 24th, 2022

DOI: https://doi.org/10.21203/rs.3.rs-1636865/v1

Abstract

Despite the extensive use of the cuprizone (CPZ) demyelination animal model, there is little evidence regarding the effects of CPZ on a cellular level. Initial studies have suggested that oligodendrocytes (OL) are the main cell targets for CPZ toxicity. However, recent data have revealed additional effects on neural stem cells and progenitor cells (NSC/NPC), which constitute a reservoir for OL regeneration during brain remyelination.

We cultured NSC/NPC as neurospheres to investigate CPZ effects on cell mechanisms which are thought to be involved in demyelination and remyelination processes *in vivo*. Proliferating NSC/NPC cultures exposed to CPZ showed overproduction of intracellular reactive oxygen species and increased progenitor migration at the expense of a significant inhibition of cell proliferation. Although NSC/NPC survival was not affected by CPZ in proliferative conditions, we found that CPZ treated cultures undergoing cell differentiation were more prone to cell death than controls. The commitment and cell differentiation towards neural lineages did not seem to be affected by CPZ, as shown by the conserved proportions of OL, astrocytes and neurons. Nevertheless, when CPZ treatment was performed after cell differentiation, we detected a significant reduction in the number and the morphological complexity of OL, astrogliosis and neuronal damage. We conclude that, in addition to damaging mature OL, CPZ also reduces NSC/NPC proliferation and activates progenitor migration. These results shed light on CPZ toxicity in the brain and could serve to understand the exhaustion of regenerative mechanisms from NSC/NPC in the chronic CPZ animal model.

Introduction

Cuprizone (CPZ) is a potent copper-chelator which induces demyelination in the rodent brain. Although its neurotoxic mechanism is only partially understood [1], it has been widely used for the study of remyelination mechanisms. CPZ treated mice exhibit extensive loss of oligodendrocytes (OL) and brain demyelination in both white and gray matter, accompanied by astrogliosis, microglial activation and neuronal degeneration [2–13]. Withdrawal of the toxic from the diet enables remyelination by the rapid activation of pre-existing oligodendroglial precursor cells (OPC) located near demyelinated areas, which proliferate and migrate short distances to give rise to new remyelinating OL [14–15]. A second mechanism was shown to equally participate in the remyelination process through *de novo* OL generation from neural stem cells and progenitor cells (NSC/NPC) niches [16–26]. These two mechanisms act in concert to balance out OL deficit and to promote remyelination. However, after exhaustion of local OPC as a source of new OL, oligodendrogenesis from NSC/NPC becomes relevant for successful remyelination. Even more, if CPZ intoxication is prolonged in time, a chronic demyelination status is reached due to the full depletion of both cell sources for remyelination [25, 27].

To better understand CPZ toxicity, a few reports have evaluated CPZ effects on several types of brain cells *in vitro*. Rat OPC-enriched cultures treated with CPZ showed the inhibition of OL maturation without affecting OPC numbers [28]. It was also suggested that microglial cells could act as mediators of CPZ

toxicity on mature OL by the production and secretion of pro-inflammatory cytokines [29]. Furthermore, Bénardais et al. [30] did not find effects on the proliferation and survival of microglia, astrocytes or OPC when glial cell cultures were treated with CPZ. In contrast, differentiated mature OL were found to be significantly affected by CPZ treatment, suggesting that the ultimate targets for CPZ toxicity are mature OL [31]. Additionally, Brousse et al. [25] have described a direct inhibitory effect of CPZ on NSC/NPC proliferation. Whether other NSC/NPC properties are affected by CPZ or not, is still unresolved.

To decipher if NSC/NPC mechanisms are directly affected by CPZ treatment, we took advantage of the neurosphere (NS) culture system as an *in vitro* approach that recapitulates some cellular processes taking place *in vivo* during remyelination. We studied CPZ effects on cellular processes known to be involved in OL generation such as NSC/NPC proliferation, progenitor migration, cell differentiation, and cell survival.

Materials And Methods

Animals and reagents

Wild type C57BL/6j mice were acquired at Facultad de Ciencias Veterinarias, UBA. C57BL/6-Tg(CAG-EGFP)1Osb/J transgenic mice expressing the enhanced green fluorescent reporter under chicken beta actin gene promoter and cytomegalovirus enhancer (ACT::GFP) (RRID:MGI:2686900, Jackson, Bar Harbor, USA), was kindly provided by Dr. Campetella (IIBIO, CONICET). All mice strains were maintained in the animal care facility at IQUIFIB- UBA-CONICET, following institutional guidelines for animal care. Protocols were in accordance with guidelines from the Comité Institucional de Cuidado y Uso de Animales de Laboratorio (CICUAL)- at Facultad de Farmacia y Bioquímica- UBA and were approved by Res (D) Nº4538/2018 and Res (D) Nº 657/2020.

Cuprizone (Bis-cyclohexanone oxaldihydrazone), poly-L-lysine, 5-bromo-2´-deoxyuridine (BrdU), bisbenzimide a33258 (Höechst), propidium iodide (PI) and Triton X-100 were purchased from Sigma-Aldrich Argentina. DMEM-F12, Hanks balanced salt solution (HBSS) and B-27 Supplement were from Gibco Life Technologies. Plasticware was acquired from Elessar (Argentina), fetal calf serum (FCS) was from Cripion SRL (Argentina). Mowiol 4-88 was from Calbiochem. Paraformaldehyde (PFA), sucrose and other reagents were from Biopack. Epidermal growth factor (EGF) was purchased from Peprotech and basic fibroblast growth factor (bFGF) was a gift from Dr Baldi (IBYME, UBA-CONICET). H_2DCFDA probe was a gift from Dr. Sandra Verstraeten (Universidad de Buenos Aires, CONICET). Primary antibodies are listed in Table 1. All secondary antibodies were purchased from Jackson ImmunoResearch.

Tissue processing and immunohistochemistry

Neonatal mice between 2-4 days old were euthanized by decapitation and brains were removed, washed in phosphate buffered saline (PBS) and fixed overnight in 4 % PFA-PBS. After rinsing in PBS, brains were sequentially set to soak in 15 % and 30 % sucrose solutions at 4 ºC and finally were frozen at -80 ºC until sectioned with a Leica CM1850 cryostat in 30 µm thick slices. Tissue sections were adhered to glass

slides and processed for immunohistochemistry (IHC). After blocking with 5 % FCS, 0.1 % Triton X-100 in PBS solution, sections were incubated overnight with primary antibodies (Table 1) diluted in PBS with 1 % FCS and 0.02 % Triton X-100. Brain slices were then rinsed in PBS and incubated with the appropriate fluorescent secondary antibodies (1:2000) together with 5 µg/ml Höechst 33258 for nuclei staining. After washing in PBS, sections were air dried and mounted with Mowiol solution.

Neurosphere cultures and treatments

For all the experiments, 2-4 days old newborn mice were sacrificed by decapitation and SVZ was removed from brains. Cell suspensions were obtained by mechanical dissociation of SVZ tissue with a P1000 micropipette tip. Cells were washed in 5 ml DMEM-F12 and after 5 min centrifugation at 300 xg, supernatant was discarded. Cell pellets were resuspended and cultured in DMEM-F12 supplemented with 2 % B-27, 20 ng/ml bFGF and 20 ng/ml EGF (proliferative medium), for maintenance of undifferentiated and highly proliferative status. Growth factors were added to the culture medium every other day. In this proliferative condition, cells retained multipotency and undifferentiation, both when cultured as NS in suspension in T25 flasks or 24-well culture plates, as well as when grown as a monolayer on poly-L-lysine-coated coverslips. Differentiation of NSC/NPC into neural lineages was induced by changing culture medium to DMEM-F12 with 2 % B-27 Supplement without growth factors (differentiating medium).

CPZ solutions at different concentrations were prepared in 50 % v/v ethanol by serial dilutions from a 6 mg/ml CPZ stock freshly prepared in ethanol 50 % v/v. Identical volumes of each CPZ working solution, representing less than 5% of final volume, was added to the culture media to reach desired final CPZ concentrations, according to the previously used reference range (Pasquini et al., 2007). For CPZ0, we added the same volume of 50% v/v ethanol without CPZ to the medium. In every experiment we run in parallel a control condition containing culture media without any treatment (CTL).

NSC/NPC viability and proliferation assays

NS were grown in suspension in proliferative media (+bFGF/EGF) containing different CPZ doses by triplicate. After one week in culture, NS were fixed in 4 % PFA and photographed at low magnification for determination of total numbers of NS and NS diameter in each condition.

For quantitation of viable cells, intact or dissociated NS from ACT::GFP mice were seeded into poly-L-lysine-coated coverslips with proliferative or differentiating media and were grown with or without CPZ, depending on the experiment. Cells were fixed with 4 % PFA and after washing in PBS, they were stained with 5 µg/ml final Höechst 33258. GFP fluorescence associated to living cells, and Höechst staining of total nuclei were observed by fluorescence microscopy.

For proliferation assay, 24 hours before fixing with 4 % PFA, cells were incubated with 10 µM 5-Bromo-2'-deoxyuridine (BrdU) and then were analyzed by immunocytochemistry using anti BrdU antibody.

NPC migration and processes elongation in proliferating cultures

Whole NS were seeded by triplicate on poly-L-lysine coated coverslips and cultured for 48 hours in proliferative conditions (+bFGF/EGF) with CPZ treatments. During this period, numerous cell processes elongate from the NS surface and individual cells detached from the NS and migrate away from the NS border. Cells were washed in PBS twice, fixed in PFA 4 % solution for 20 min at room temperature and subjected to immunocytochemistry and Höechst staining. After culture images were taken, the outline of individual NS was manually demarcated to establish NS border. For each condition we selected NS which met the requirement of being isolated (without interaction with neighboring NS). For each NS, we determined the external edge/border of migratory cells to include all $GFAP^+$ cell processes and Höechst-stained cell nuclei arising from the central NS to demarcate the complete migratory area. This area was subdivided in concentrical rings every 50 µm. We registered nuclei numbers inside each migratory ring. We also measured NS diameter and the maximal length of the external edge containing cells processes from individual NS.

Cell differentiation and cell death analysis

Cell suspensions from dissociated NS cultures were seeded onto poly-L-lysine-coated coverslips and were left one hour for adhesion. Cell differentiation was started by adding differentiating media (without bFGF/EGF) with CPZ treatments by triplicate. Cells were differentiated for one week and then they were washed twice in PBS, fixed in PFA 4% solution for 20 min at room temperature and finally rinsed in PBS. Cell differentiation was evaluated by immunocytochemistry for oligodendrocytes, astrocytes, neurons, or progenitors by detection of specific markers (see immunocytochemistry section). For cell death analysis, cells were incubated with propidium iodide 100 µg/ml before fixation for 30 min.

CPZ effects on mature oligodendrocytes, astrocytes, and neurons survival

Dissociated NS were seeded on coverslips and grown for six days in proliferative media. Then, media was switched to differentiating conditions (without mitogens) without any treatment and cultured for six days. Once differentiated, cells were exposed to CPZ treatments by triplicate for two additional days. Immunocytochemical analysis was performed to detect oligodendrocytes, astrocytes, neurons and oligodendroglial precursors. For each marker, one coverslip was removed before CPZ treatment was started, as a control for initial cell proportions as the pre-treatment condition (PRE).

Immunocytochemistry

PFA-fixed cells were blocked with 5% FCS– 0.1% Triton X-100 in PBS solution and incubated with primary antibodies listed in table 1. For BrdU immunodetection, antigen retrieval was performed after fixation by incubation with 2 N HCl for 20 min at 37 º C, followed by neutralization with 0.1 M Sodium Borate (pH 9) for 15 min at 37 º C and a blocking step overnight with 2 % FCS.

All antibodies were diluted in a 1% FCS, 0.02% Triton X-100 in PBS solution and incubated overnight at 4 ºC. After rinsing in PBS, cells were incubated with the appropriate secondary antibody (Jackson IR, 1:2000) together with Höechst 33258 for nuclei staining at 5 µg/ml. We performed red and green

detection for two markers in cell cultures derived from wild type animals combined with blue nuclei Höechst staining. In some experiments in which NS were generated from ACT::GFP mice, green channel was reserved for GFP detection as a control for cell viability and only one additional marker was evaluated using a secondary antibody with red fluorophore by immunocytochemistry.

Determination of intracellular ROS

For oxidative stress determination, intracellular ROS levels were monitored by using (6)-carboxy-2´,7´-dichlorodihydrofluorescein diacetate probe (H_2DCFDA) (Molecular Probes Inc., Cat #C-400), which is converted into a fluorescent compound (DCF) upon oxidation with ROS. Internalization of the probe into cells was confirmed by fluorescence microscopy. Briefly, NS were dissociated, and cells were attached to poly-L-lysine coated coverslips and cultured in proliferative conditions for six days. CPZ treatments were performed for 24 hours and then the medium was removed and replaced with HBSS containing 5 μM H_2DCFDA probe. After 30 min of incubation at 37 ºC under 5 % of CO_2, medium was discarded, and cells were rinsed twice with PBS and immediately photographed under a fluorescence microscope.

For quantitative analysis of DCF fluorescence, cells attached to 96-well plates were cultured in proliferative conditions for six days. At the end of this period, cells were treated with different CPZ doses for 3, 6, 9, 24, 48, or 72 hours. Medium from each well was removed and replaced with HBSS containing 5 μM H_2DCFDA probe. After 30 min of incubation at 37 ºC under 5 % of CO_2, medium was discarded, and cells were rinsed twice with PBS. Nuclei were dyed with 5 μM Höechst 33258, and fluorescence was monitored in a plate reader fluorometer (Flexstation 3, Molecular Devices) at 485 nm excitation and 535 nm emission wavelengths. The experiment included six replicates for each condition and was performed three times.

ROS determination by flow cytometry was performed both in proliferative and differentiating cultures. Wild type mice-derived NS were dissociated and seeded in poly-L-lysine-coated 24 well plates. For proliferative cultures, cells were grown in a proliferative medium for 6 days and then treated with CPZ for 24 hours. Culture medium was discarded, and cells were incubated with 5 μM H_2DCFDA probe in HBSS for 30 min at 37 º C under 5 % of CO_2. Cells were harvested and resuspended in PBS with 5 mM EDTA. Flow cytometry was performed using a Pas III flow cytometer (Partec, Germany). Background fluorescence intensity was determined in control cells in which incubation with the probe was omitted. Analysis of data was performed with FlowJo v10.0.8 software (FlowJo, Ashland, OR, USA) after excluding doublets and dead cells. For differentiating cultures, dissociated cells were cultured for 6 days in proliferative conditions and 6 additional days in differentiating medium. After treatment with CPZ for 24 hours, culture medium was discarded, and cells were incubated with 1 μM H_2DCFDA probe in HBSS for 30 min at 37º C under 5% of CO_2, and further processed for flow cytometry as for proliferative cultures.

Morphological analysis of oligodendrocytes

To examine morphological complexity of MBP^+ mature oligodendrocytes, we compared high magnification images of cultures treated after differentiation with CPZ500 and CPZ0. Analysis was performed with ImageJ RRID:SCR_003070 https://imagej.net/. OL processes were outlined with NeuronJ plugin and Sholl analysis was employed to set a ring grid centered in the cell soma (starting radius: 10 μm; step size: 10 μm; end: 200 μm) as previously reported [32]. The number of process crossings per ring for at least 15 MBP^+ cells were determined from each condition. Mean total process crossings per ring was plotted against the distance from OL soma of the corresponding ring.

Image acquisition

Images were captured with an Olympus BX50 fluorescence microscope (RRID:SCR_018838) and a DP73 digital camera (Olympus, RRID:SCR_017564) with the CellSens software (RRID:SCR_014551). Cell quantification, and image measurements were performed using Image-Pro Plus (RRID:SCR_007369, http://www.mediacy.com/imageproplus). Low magnification images for determination of NS size were acquired with a Nikon Elipse TE300 inverted microscope and for the total numbers of NS we used a Leica EZ4 stereomicroscope and a Kodak Easy Share Camera.

Statistical analysis

Statistical analysis was performed by using GraphPad Prism software (RRID:SCR_002798, http://www.graphpad.com/). Statistical tests are indicated in figure legends and significance is represented as ***p<0.001; **p<0.01; *p<0.05, bars without asterisks or indicated as *ns* correspond to non-significant differences.

Results

Characterization of the NS culture system

To characterize the mice brain tissue that was used to generate NS cultures, we first explored the *in vivo* expression of several neural markers at 2-4 postnatal days (P2-P4) (Fig. 1). Neural stem cells and neural progenitor cells (NSC/NPC) marker Sox2 was strongly expressed in subventricular zone (SVZ) cells. We also detected scattered $Sox2^+$ cells in surrounding tissues of corpus callosum and caudate putamen (Fig. 1b). Contrarily, GFAP expression was prominent in astrocytes within the corpus callosum but only scarcely detected in cells of the ventricle walls (Fig. 1c). Other glial precursors and oligodendroglial lineage markers expressed at different OL maturation stages, identified by Olig2, Sox2, PDGFRα and NG2 expression, were found dispersed in the corpus callosum and caudate putamen with some positive cells located in ventricular walls (Fig. 1d-g).

For NS generation, NSC/NPC were amplified from SVZ of 2-4 days old animals as shown in Fig. 2a. Under proliferative and non-adherent conditions, these cells can proliferate and remain attached to each other, forming NS. After one week in culture, NS size reached 80-100 μm in diameter (Fig. 2b). We studied NS behavior under different culture conditions over time to optimize the procedures for subsequent analysis.

For migration studies, intact control NS were adhered to poly-L-lysine-coated coverslips and maintained in proliferative media. After one day in culture, GFAP expression was detected in some cells of the NS (Fig. 2c). A strong upregulation of $GFAP^+$ cell numbers and the elongation of $GFAP^+$ radial cell processes were observed after 2-4 days in this culture conditions (Fig. 2d). Alternatively, floating NS were dissociated and cultured as adherent two-dimensional monolayer for six days (Fig. 2e). If mitogens were added to the media during this 6-day period, the cells remained in an undifferentiated state as demonstrated by the expression of Sox2 NSC/NPC marker (green in Fig. 2e). In these proliferative conditions, we found that 80 % of $Sox2^+$ cells incorporate BrdU after a 24 hours pulse (red in Fig. 2e). Immunocytochemical analysis revealed that NS cultures contain no contaminating $CD11b^+$ microglia or MBP^+ mature oligodendrocytes (not shown). Only few $Tuj1^+$ neuroblasts were detected in proliferating cultures (not shown). Withdrawal of mitogens from culture medium promoted cell differentiation. After six days in differentiating medium (Fig. 2f-i), multipotency of NS cultures was demonstrated by the detection of cells of the three neural lineages: $Tuj1^+$ neurons (red in Fig. 2f), $GFAP^+$ astrocytes (red in Fig. 2g) and MBP^+ mature OL (green in Fig. 2h), in proportions of 8 %, 20 % and 3 %, respectively. Although MBP^+ mature OL represent a very low proportion of the cells in differentiated cultures, numerous $Sox10^+$ cells belonging to the oligodendroglial lineage were detected (green in Fig. 2f). The finding of substantial numbers of $PDGFR\alpha^+$ oligodendroglial precursor cells (OPC) (green in Fig. 2g) and Carbonic anhydrase II^+ (CAII) immature OL (red in Fig. 2h) confirmed that several OL lineage cells at different maturity phases were simultaneously present in differentiated cultures. Furthermore, the marker for glial progenitors A2B5 was also detected (red in Fig. 2i). As expected, differentiating cultures exhibit only 20 % of cells expressing Sox2 (not shown). We observed that many $GFAP^+$ cells with an astrocyte-like morphology co-expressed PDGFRα (Fig. 2g), indicating that this marker is not exclusively expressed by OPC in these culture conditions as previously reported [33].

We simultaneously took advantage of ACT::GFP mice-derived NS, as they were previously reported to be equivalent to that from wild type mice, in terms of their behavior in culture [34]. We generated ACT::GFP-derived NS and confirmed the same $Sox2^+$ $GFAP^+$, MBP^+ and $Tuj1^+$ cell proportions as in wild type NS cultures both in proliferative and differentiating conditions (not shown). We detected constitutive expression of GFP in 100 % of the cells when ACT::GFP-derived NS were adhered and cultured for two days in proliferative media (Fig. 3a-c). After NS dissociation and culturing in differentiating media, GFP was still expressed in cells. However, we detected some pyknotic nuclei lacking GFP expression (Fig. 3d-f, open arrowheads). We found that the constitutive expression of GFP was a suitable viability marker since it was exclusively restricted to living cells and excluded from propidium $iodide^+$ (PI^+) dead cells (Fig. 3g-l, arrowheads). This was particularly useful for the experiments performed during the differentiation period, when cell death was more pronounced.

CPZ treatment reduces NS proliferation without affecting NSC/NPC survival

To study if CPZ affects NSC/NPC viability and proliferation, different doses of CPZ were added to proliferative media throughout the process of NS generation in suspension from periventricular wild type

mice brain cells. After six days in culture, we detected the formation of NS in all the studied conditions (Fig. 4a-h). The survival of the initial NSC/NPC was determined by their ability to generate NS. Thus, we registered the number of NS formed in each condition. We did not find differences in NS numbers between CPZ-treated cultures and controls, suggesting that initial NSC/NPC viability was not affected by CPZ (Fig. 4i).

We indirectly estimate NSC/NPC proliferation rate by determining NS size in each condition as previously reported [35-36]. We detected a significant reduction in NS diameter in response to CPZ treatment at concentrations from 500 μM (Fig. 4j). To reinforce these results, we performed a BrdU proliferation assay. We found a 50 % reduction in the percentage of $BrdU^+$ cells in cultures treated for six days with CPZ1000 compared to CPZ0 (Fig. 4k-m), confirming that NSC/NPC proliferation was inhibited by CPZ treatment.

CPZ treatment induces cell migration from NS

Migration of cells from NS involves an organized cell pattern in which long $GFAP^+$ processes serve as a scaffold for numerous progenitors that detach from NS and move outwards in a radial fashion (Fig. 5a, b, d, e). Whole NS from wild type mice were adhered to poly-L-lysine-coated coverslips and exposed to CPZ in proliferative media for two days. Ten to fifteen NS from each condition were analyzed to study cell migration patterns. GFAP immunofluorescence was performed to demarcate NS outline and the outer limit of $GFAP^+$ processes to set the area of analysis for migratory nuclei (dotted line in Fig. 5a, b, d and e). The radius of the migratory area was increased in CPZ1000 treated cultures compared to CPZ0 (Fig. 5c). Quantification of total nuclei inside the area of analysis for each NS showed higher numbers of migratory cells in response to CPZ treatment (Fig. 5f). Furthermore, we selected a sector of the migration area (Fig. 5g-h) and measured the distance for each nucleus to the NS edge (dotted lines from individual cells in Fig. 5h). We found that average migration distance of nuclei detached from NS was also expanded in the CPZ1000 condition compared to CPZ0 treated cultures (Fig. 5i). These findings are summarized in the heatmap graphs showing nuclei distribution profiles from representative CPZ0 and CPZ1000 treated NS (Fig. 5j-k).

CPZ treatment induces oxidative stress

As CPZ effects *in vivo* have been associated with oxidative stress induction and ROS- mediated injury [1, 37], we evaluated if CPZ *in vitro* effects on cell proliferation and cell migration could be accompanied by increased intracellular oxidative stress levels. By using H_2DCFDA probe (Fig. 6a) and fluorescence microscopy we first confirmed the internalization of the probe and fluorescence emission by DCF product after 24 hours of CPZ treatment in NS-dissociated cells grown in proliferative medium (Fig. 6b, c). Quantification of DCF fluorescence by using a multi-plate reader fluorometer revealed that ROS levels were increased in a dose dependent manner after exposure to CPZ for 24 hours (Fig. 6d). The status of oxidative stress in cells was evaluated after 3 to 72 hours of CPZ treatment. Fluorometric determination of DCF showed that CPZ1000 produced the strongest effect on intracellular ROS levels after 24 hours treatment (Fig. 6e). Analysis by flow cytometry confirmed that ROS levels were increased after 24 hours

treatment in CPZ1000 compared to CPZ0 cultures, as the percentages of cells with high and medium levels of intracellular ROS were augmented at the expense of the reduction in cells with low-ROS levels (Fig. 6f-g). Comparison of the proportions DCF^+ cells between CPZ0 and CPZ1000 showed that cells with higher ROS levels were incremented from 6.32 to 12.6 %, cells with intermediate ROS values increased from 48.8 to 62.4 % and cells with low ROS signal were reduced from 44.9 to 25 %. CPZ1000 upregulation on ROS production was even higher than the hydrogen peroxide positive control (Fig. 6h).

CPZ effects on cell differentiation towards neural lineages

To examine the effects of CPZ during the process of cell differentiation, dissociated ACT::GFP NS were seeded on poly-L-lysine-coated coverslips and cultured for 24 hours in DMEM/F12 + B-27 with the addition of mitogens. Then, one batch of cells was separated and fixed as the proliferation control (Fig. 7a), and the rest were differentiated by switching culture media to DMEM/F12 + B-27 without mitogens with the addition of CPZ treatments. After six days, we observed a 30 % reduction in the percentage of GFP expressing cells in control differentiating cultures compared to the initial condition before differentiation (Fig. 7b, c). The reduction in the percentage of living cells was more pronounced when cultures were treated with CPZ, reaching survival rates near 30 % at 1000 µM CPZ (Fig. 7c). Despite the general cytotoxic effect exhibited by higher doses of CPZ during differentiation phase, remaining cells were able to differentiate into MBP^+ OL (Fig. 7d, g), $Tuj1^+$ neurons (Fig. 7e, h) and $GFAP^+$ astrocytes (Fig. 7f, i). We found that the proportions for mature OL (3 %), neurons (8 %) or astrocytes (20 %), relativized to GFP^+ viable cells, were not significantly affected by CPZ treatment (Fig. 7j-l). Besides the susceptibility of NS-derived cells during the process of cell differentiation that leads to a decrease in cell viability, our results indicate that CPZ deepens this effect without affecting any particular neural lineage proportion. Contrary to the effects of CPZ found on proliferating cultures, flow cytometry analysis revealed that intracellular ROS levels were not affected by CPZ treatment in differentiating cultures (Fig. 7m, n). Similar cell proportions were obtained when NS ability to differentiate into neural lineages was evaluated in wild type mice-NS derived cells (Fig. 7o). As our main interest was centered on OL and due to the low proportion of MBP^+ OL detected in differentiating cultures (Fig. 7j), we attempted to improve general cell survival and to increase the total number of mature OL by adding FCS to the culture medium during the differentiation period. However, although under this condition cultures reached cell survival rates near 90-100 % at all CPZ concentrations, FCS promoted cell differentiation towards astrocytes, and did not increase the numbers of OL as expected (Fig. 7p).

Effects of CPZ on mature differentiated cells

To study if CPZ affects mature OL, differentiated cultures were generated from ACT::GFP-derived NS. After dissociation, cells were maintained in differentiating media during six days without any treatment. After cell differentiation occurred, one coverslip by triplicate was fixed as the pre-treatment condition (PRE) (Fig. 8a-b) and the rest of the wells were treated with CPZ for two additional days (schematized in Fig. 8c). Immunofluorescence for MBP revealed that mature OL numbers were reduced by CPZ treatment in a dose dependent manner (Fig. 8d-m). CPZ1000 was excluded from the analysis, as no MBP^+ OL were

detected in this condition. GFP$^+$ living cells relativized to total nuclei show similar percentages at all the tested CPZ doses suggesting that general cell survival of differentiated cells was not significantly affected by CPZ (Fig. 8n).

Quantification of MBP$^+$ mature OL showed a 40 % reduction in the percentages of OL in control cultures differentiated for eight days compared to the initial control cells differentiated for six days (Fig. 8o, CTL and CPZ0 vs PRE). Furthermore, we found a significant reduction in OL percentages in cultures exposed to CPZ at 100 and 500 μM, compared to CPZ0 (Fig. 8o).

Intact adhered ACT::GFP-derived NS were also treated after the differentiation period to confirm whether OL were affected by CPZ in the context of the more complex tridimensional NS structure. After cell differentiation, cultures were treated with CPZ0 or CPZ500 in differentiating media for two days. Immunofluorescence analysis confirmed OL loss triggered by CPZ500 treatment in comparison to CPZ0 (Fig. 8p-q). Besides the reduction in the number of mature OL, we found that morphological complexity of OL was affected as well by CPZ in differentiated cultures (Fig. 9a-d). Sholl analysis of individual OL revealed a significant drop in the number of OL ramifications in CPZ500-treated cultures compared to CPZ0 (Fig. 9e). Immunocytochemistry for several markers was performed to evaluate whether CPZ affects other neural lineages in dissociated cultures after differentiation (Fig. 10). Cells differentiated for eight days in control media (CTL) were compared to cells differentiated for six days and treated for two additional days (CPZ0 and CPZ500, Fig. 10a, b, c). Results revealed that the percentage of Tuj1$^+$ neuroblasts was triplicated during this short two-day period in differentiating conditions (Fig. 10a), while proportions of both GFAP$^+$ (Fig. 10b), as well as PDGFRα$^+$ cells (Fig. 10c) were mildly reduced. CPZ500 treatment did not seem to affect the number of neurons, as differences in the percentages of Tuj1$^+$ cells between CPZ0 and CPZ500 were not significant (Fig. 10a). On the contrary, the proportions of GFAP$^+$ (Fig. 10b) and PDGFRá$^+$ cells (Fig. 10c) were slightly increased in CPZ500 respect to CPZ0. We also identified some morphological cell features at the qualitative level when CPZ500-treated NS were compared to CPZ0 condition. The reduced morphological complexity of MBP$^+$ mature OL in CPZ500 condition was accompanied by a higher proportion of bipolar PDGFRα$^+$ OL precursors (Fig. 10d-e). We also found hypertrophic GFAP$^+$ astrocytes in CPZ500 treated cultures (Fig. 10f, g) as well as highly affected Tuj1$^+$ neurons, which exhibit shorter neurites in comparison to CPZ0, with some evident signs of damage (Fig. 10 f, g).

Discussion

Multiple Sclerosis is the most prevalent demyelinating disease in humans. Even though CPZ intoxication in animals is the most frequently used model to study nonautoimmune mediated demyelination and spontaneous remyelination [3, 37–39], only a few reports have explored *in vitro* CPZ toxic effects on OL [28–30]. Additionally, it has been shown that proliferation of neural stem cells is another target for CPZ toxicity [25].

Here, we took advantage of the *in vitro* NS culture model to study whether NSC/NPC behavior is directly affected by CPZ treatment. Periventricular tissue at 2–4 postnatal days, used for NS generation, is an enriched source for Sox2 + multipotent NSC/NPC. Although identification of NSC/NPC is somehow difficult, as they exhibit heterogeneous marker expression profiles, Sox2 was shown to be a suitable marker to detect NSC/NPC throughout lifespan [40–43]. In contrast to adult SVZ, we did not detect GFAP expression in NSC/NPC of 2–4 days old mice. As previously reported, *in vivo* appearance of GFAP expression in SVZ is initiated at postnatal days 6–7 and remains throughout adult life as a source for multipotent neural progenitors [44–46]. Olig2, Sox2, PDGFRα and NG2 oligodendroglial lineage markers showed a minor contribution to neonatal SVZ.

Due to heterogeneous data referring to cell composition of NS grown in different culture conditions [47], it was first necessary to characterize NS cultures to determine cell proportions and their behavior in response to the experimental protocol. Our results showed that GFAP expression is strongly activated in NS after a few days in culture, mimicking the *in vivo* temporal expression of GFAP. Both floating NS as well as 2D adherent monolayers cultured in proliferating media showed sustained expression of Sox2 and GFAP, retained multipotency and displayed high levels of proliferation by BrdU incorporation as previously reported [48–49]. Although there is some controversy on whether a subset of NSC expresses PDGFRα *in vivo* or not [50–52] in our hands, many GFAP + astrocytes in dissociated NS cultures co-expressed PDGFRα.

Withdrawal of growth factors from the medium slowed down cell proliferation and triggered cell differentiation, so that NS-derived cells differentiated into lineage-specific precursors and fully differentiated cells. In our culture conditions, differentiation into mature oligodendrocytes and neurons was limited, as both lineages represent a minor proportion of cells. Meanwhile, astrocytes constitute 20% of the cells in the culture after six days in differentiating conditions. Furthermore, other oligodendroglial precursors such as PDGFRα$^+$ cells were detected both in proliferating and differentiated cultures, showing that in addition to self-renewing cell population and mature cells, NS-derived cultures reproduce, at least in part, the cellular diversity of brain tissue.

Neonatal brain-derived NS, although initially different to NS originated from older animals [53], can recapitulate most of the processes known to occur during *in vivo* remyelination, such as proliferation, cell migration, cell commitment, differentiation to neural lineages and cell maturation, and serves as a model for reproducing some key features of the remyelination process [49]. Additionally, they grow fast in the presence of mitogens and can be amplified in large numbers, making NS generation easier and less time consuming than their older NSC/NPC-derived counterparts.

Here we showed that CPZ treatment did not affect survival of NSC/NPC, as similar numbers of NS were generated at all CPZ doses. Contrarily, the reduction in NS size in a dose dependent manner as well as the decrease in BrdU incorporation are consistent with previous findings showing that CPZ treatment inhibits NSC/NPC proliferation [25]. It is interesting to highlight that demyelination in the *in vivo* CPZ model is characterized by the upregulation of NSC proliferation in the SVZ, which contributes with migratory

progenitors for remyelination [9, 54]. However, our findings demonstrating that CPZ acts by directly inhibiting NSC/NPC proliferation, suggest that SVZ proliferation *in vivo* might be activated by other signals associated with demyelination. Moreover, our results could explain the failure of brain remyelinating ability in the *in vivo* chronic model by the exhaustion of remyelinating cells from SVZ source after long-term CPZ inhibition on NSC proliferation.

We found that the length of $GFAP^+$ radial glia-like cell processes increased after CPZ treatment. This finding exhibits some resemblance to that observed during SVZ activation after CPZ administration *in vivo* [9]. The number of NS-derived migratory cells was augmented as well, suggesting that CPZ is somehow promoting mechanisms driving cell migration. In line with these results, we found that CPZ incremented intracellular ROS production in proliferating NS cells. *In vivo*, NSC/NPC have a high basal ROS production and a very active antioxidant machinery, compared to other more differentiated cell types [55]. In a context in which NSC/NPC proliferation is robust, increased ROS levels after exposure to CPZ could be attributed to the copper chelation and the inhibition of several copper-dependent detoxifying enzymes, as previously suggested [1, 37, 56–58]. Furthermore, NSC/NPC appear to be particularly sensitive to changes in redox status because ROS are required for normal NSC/NPC self-renewal, but ROS overproduction can lead to mitochondrial dysfunction, depletion of ATP and inhibition of cell proliferation [59, 60]. As described for several types of stem cells [61, 62], ROS could have additional signaling roles that might impact in NSC/NPC behavior by arresting cell proliferation and triggering progenitor migration.

Contrary to the findings in proliferating cultures, cell differentiation into neural lineages was not significantly affected by CPZ treatment. We had to deal with two converging issues in differentiating cultures. On the one hand, general cell death was prominent after mitogens removal. We found that the use of ACT::GFP mice-derived NS was a suitable tool for the identification of living cells in differentiating cultures. In this way, it was more accurate to quantify astrocytes, neurons, and oligodendrocytes with respect to GFP positive living cells, instead of normalizing numbers to total nuclei, which included both living and dead cells. On the other hand, differentiated cultures showed a low proportion of OL, which complicated the analysis of this lineage. Even though cells were grown in the presence of FCS to increase viable cells and improve OL quantification, a strong commitment towards astroglial lineage was observed after FCS exposure, and OL numbers remained negligible [63, 64]. Not only was lineage commitment similar between control and CPZ-treated cultures undergoing differentiation, but also intracellular ROS levels were invariable as well.

When CPZ treatments were performed on post-differentiated NS cultures, we found that both the numbers of MBP + OL as well as their morphological complexity were affected by CPZ. The fact that mature OL are post-mitotic cells, suggests that CPZ directly affects their survival. These findings agree with CPZ toxic effects reported on OL *in vitro* [31] and *in vivo* [1, 3]. The effects of CPZ were evaluated in other neural lineages in post-differentiated cultures. Although CPZ treatment did not increment the percentages of astrocytes, OL precursors or neurons, considerable morphological alterations were found, indicating additional CPZ effects in these cell types.

Our results showed that CPZ prevents proliferation of NSC/NPC, without affecting their commitment and differentiation into neural lineages. It is tempting to speculate that CPZ-mediated free radicals overproduction might be associated with the high energy demand and the failure in the antioxidant machinery in proliferating NSC/NPC-enriched cultures. CPZ-mediated inhibition of NSC proliferation, the stimulation of progenitor's migration, and the strong toxic CPZ effect on mature OL could together explain the *in vivo* depletion of OL and the exhaustion of remyelination mechanisms in the chronic CPZ model.

CPZ-treated NS cultures reproduced several features triggered during CPZ-induced demyelination *in vivo* (Fig. 11). We could hypothesize that CPZ acts on several cell types and affects different cell processes. A direct CPZ damage on mature OL could act as the signal for the activation of the oligodendrogenic pathway from NSC/NPC (Fig. 11a). Additional direct or indirect effects of CPZ could affect other differentiated cells, leading to astrogliosis or neuronal damage. On the other hand, CPZ might inhibit NSC/NPC proliferation and trigger the activation of progenitor migration, probably by the overproduction of free radicals (Fig. 11b). Cells of the three neural lineages seem to be equally susceptible to CPZ toxicity during the process of cell differentiation. All these findings could explain remyelination failure in the chronic CPZ *in vivo* model of demyelination. Due to the dynamic complexity and overlap of demyelination/remyelination that hamper toxicity studies *in vivo*, the NS culture system presented here can be used to study individual cell mechanisms and contributes to deepen our understanding of the CPZ model.

Declarations

Acknowledgments

We would like to thank Jimena Confessore for the artwork, Francisco Dores Piuma for support with data processing, Marianela Vence for animal care and handling and Dr. Juana María Pasquini and Dr. Sandra Verstraeten for sharing laboratory reagents. Data available on request from the authors.

Funding

This work was supported by CONICET (Grant number PIP-CONICET 11220150100289CO to PF, PIP-CONICET 11220200101280CO to P.F.) and Universidad de Buenos Aires (UBACYT Grant number 200201190100048BA to P.F.)

Competing Interests

The authors have no competing interests to declare that are relevant to the content of this article.

Authors Contributions

All authors contributed to the study conception and design. Material preparation, data collection and analysis were performed by Yamila Azul Molinari and Agustín Jesús Byrne. The first draft of the

manuscript was written by Paula Gabriela Franco and all authors commented on previous versions of the manuscript. All authors read and approved the final manuscript.

Data Availability

The datasets generated during and/or analyzed during the current study are available from the corresponding author on reasonable request.

Ethics approval

This study was performed in line with the principles

All protocols in this study were approved by the local committee on animal research and ethics at Facultad de Farmacia y Bioquímica- UBA (Comité Institucional de Cuidado y Uso de Animales de Laboratorio - CICUAL) in accordance with international guidelines by Resolutions (D) Nº4538/2018 and (D) Nº 657/2020.

Consent to participate

Not applicable

Consent to publish

Not applicable

References

1. Praet J, Guglielmetti C, Berneman Z, Van der Linden A, Ponsaerts P (2014) Cellular and molecular neuropathology of the cuprizone mouse model: Clinical relevance for multiple sclerosis. Neurosci Biobehav Rev 47, 485–505. https://doi.org/10.1016/j.neubiorev.2014.10.004
2. Hiremath MM, Saito Y, Knapp GW, Ting JPY, Suzuki K, Matsushima GK (1998) Microglial/macrophage accumulation during cuprizone-induced demyelination in C57BL/6 mice. J Neuroimmunol 92(1–2), 38–49. https://doi.org/10.1016/S0165-5728(98)00168-4
3. Torkildsen O, Brunborg LA, Myhr KM, Bø L (2008) The cuprizone model for demyelination. Acta Neurol Scand Suppl 188:72–76. https://doi.org/10.1111/j.1600-0404.2008.01036.x
4. Norkute A, Hieble A, Braun A, Johann S, Clarner T, Baumgartner W, Beyer C, Kipp M (2009) Cuprizone treatment induces demyelination and astrocytosis in the mouse hippocampus. J Neurosci Res 87(6), 1343–1355. https://doi.org/10.1002/jnr.21946
5. Groebe A, Clarner T, Baumgartner W, Dang J, Beyer C, Kipp M (2009) Cuprizone treatment induces distinct demyelination, astrocytosis, and microglia cell invasion or proliferation in the mouse cerebellum. Cerebellum 8(3), 163–174. https://doi.org/10.1007/s12311-009-0099-3

6. Kipp M, Clarner T, Dang J, Copray S, Beyer C (2009) The cuprizone animal model: New insights into an old story. Acta Neuropathol 118(6), 723–736. https://doi.org/10.1007/s00401-009-0591-3
7. Buschmann JP, Berger K, Awad H, Clarner T, Beyer C, Kipp M (2012) Inflammatory response and chemokine expression in the white matter corpus callosum and gray matter cortex region during cuprizone-induced demyelination. J Mol Neurosci 48(1), 66–76. https://doi.org/10.1007/s12031-012-9773-x
8. Skripuletz T, Lindner M, Kotsiari A, Garde N, Fokuhl J, Linsmeier F, Trebst C, Stangel M (2008) Cortical demyelination is prominent in the murine cuprizone model and is strain-dependent. Am J Pathol 172(4), 1053–1061. https://doi.org/10.2353/ajpath.2008.070850
9. Silvestroff L, Bartucci S, Soto E, Gallo V, Pasquini J, Franco P (2010) Cuprizone-Induced demyelination in CNP::GFP transgenic mice. J Comp Neurol 518(12), 2261–2283. https://doi.org/10.1002/cne.22330
10. Silvestroff L, Bartucci S, Pasquini J, Franco P (2012a) Cuprizone-induced demyelination in the rat cerebral cortex and thyroid hormone effects on cortical remyelination. Exp Neurol 235 (2012) 357–367. doi:10.1016/j.expneurol.2012.02.018
11. Koutsoudaki PN, Skripuletz T, Gudi V, Moharregh-Khiabani D, Hildebrandt H, Trebst C, Stangel M (2009) Demyelination of the hippocampus is prominent in the cuprizone model. Neurosci Lett 451(1), 83–88. https://doi.org/10.1016/j.neulet.2008.11.058
12. Gudi V, Gingele S, Skripuletz T, Stangel M (2014) Glial response during cuprizone-induced de- and remyelination in the CNS: lessons learned. Front Cell Neurosci 8, 73. https://doi.org/10.3389/fncel.2014.00073
13. Zhang Y, Cai L, Fan K, Fan B, Li N, Gao W, Yang X, Ma J (2019) The Spatial and Temporal Characters of Demyelination and Remyelination in the Cuprizone Animal Model. Anat Rec (Hoboken) 302(11), 2020–2029. https://doi.org/10.1002/ar.24216
14. Franklin RJ, Gilson JM, Blakemore WF (1997) Local recruitment of remyelinating cells in the repair of demyelination in the central nervous system. J Neurosci Res 50(2), 337–344. https://doi.org/10.1002/(SICI)1097-4547(19971015)50:2<337::AID-JNR21>3.0.CO;2-3
15. Gensert JM, Goldman JE (1997) Endogenous progenitors remyelinate demyelinated axons in the adult CNS. Neuron 19(1), 197–203. https://doi.org/10.1016/S0896-6273(00)80359-1
16. El Waly B, Macchi M, Cayre M, Durbec P (2014) Oligodendrogenesis in the normal and pathological central nervous system. Front Neurosci 8, 145. https://doi.org/10.3389/fnins.2014.00145
17. Lim DA, Alvarez-Buylla A (2014) Adult neural stem cells stake their ground. Trends Neurosci 37(10), 563–571. https://doi.org/10.1016/j.tins.2014.08.006
18. Aguirre A, Dupree JL, Mangin JM, Gallo V (2007) A functional role for EGFR signaling in myelination and remyelination. Nat Neurosci 10(8), 990–1002. https://doi.org/10.1038/nn1938
19. Cayre M, Bancila M, Virard I, Borges A, Durbec P (2006) Migrating and myelinating potential of subventricular zone neural progenitor cells in white matter tracts of the adult rodent brain. Mol Cell Neurosci 31(4), 748–758. https://doi.org/10.1016/j.mcn.2006.01.004

20. Menn B, Garcia-Verdugo JM, Yaschine C, Gonzalez-Perez O, Rowitch D, Alvarez-Buylla A (2006) Origin of oligodendrocytes in the subventricular zone of the adult brain. J Neurosci 26(30), 7907–7918. https://doi.org/10.1523/JNEUROSCI.1299-06
21. Nait-Oumesmar B, Decker L, Lachapelle F, Avellana-Adalid V, Bachelin C, Baron-Van Evercooren A (1999) Progenitor cells of the adult mouse subventricular zone proliferate, migrate and differentiate into oligodendrocytes after demyelination. Eur J Neurosci 11(12), 4357–4366. https://doi.org/10.1046/j.1460-9568.1999.00873.x
22. Picard-Riera N, Decker L, Delarasse C, Goude K, Nait-Oumesmar B, Liblau R, Pham-Dinh D, Baron-Van Evercooren A (2002) Experimental autoimmune encephalomyelitis mobilizes neural progenitors from the subventricular zone to undergo oligodendrogenesis in adult mice. Proc Natl Acad Sci U S A 99(20), 13211–13216. https://doi.org/10.1073/pnas.192314199
23. Jablonska B, Aguirre A, Raymond M, Szabo G, Kitabatake Y, Sailor KA, Ming GL, Song H, Gallo V (2010) Chordin-induced lineage plasticity of adult SVZ neuroblasts after demyelination. Nat Neurosci 13(5), 541–550. https://doi.org/10.1038/nn.2536
24. Ortega FB, Konstabel K, Pasquali E, Ruiz JR, Hurtig-Wennlöf A, Mäestu J, Löf M, Harro J, Bellocco R, Labayen I, Veidebaum T, Sjöström M (2013) Objectively Measured Physical Activity and Sedentary Time during Childhood, Adolescence and Young Adulthood: A Cohort Study. PLoS One 8(4). https://doi.org/10.1371/journal.pone.0060871
25. Brousse B, Magalon K, Durbec P, Cayre M (2015) Region and dynamic specificities of adult neural stem cells and oligodendrocyte precursors in myelin regeneration in the mouse brain. Biol Open 4(8), 980–992. https://doi.org/10.1242/bio.012773
26. Butti E, Bacigaluppi M, Chaabane L, Ruffini F, Brambilla E, Berera G, Montonati C, Quattrini A, Martino G (2019) Neural stem cells of the subventricular zone contribute to neuroprotection of the corpus callosum after cuprizone-induced demyelination. J Neurosci 39(28), 5481–5492. https://doi.org/10.1523/JNEUROSCI.0227-18.2019
27. Skripuletz T, Gudi V, Hackstette D, Stangel M (2011) De- and remyelination in the CNS white and grey matter induced by cuprizone: The old, the new, and the unexpected. Histol Histopathol 26(12), 1585–1597. https://doi.org/10.14670/HH-26.1585
28. Cammer W (1999) The neurotoxicant, cuprizone, retards the differentiation of oligodendrocytes *in vitro*. J Neurol Sci 168(2), 116–120. https://doi.org/10.1016/S0022-510X(99)00181-1
29. Pasquini LA, Calatayud CA, Bertone Uña AL, Millet V, Pasquini JM, Soto EF (2007) The neurotoxic effect of cuprizone on oligodendrocytes depends on the presence of pro-inflammatory cytokines secreted by microglia. Neurochem Res 32(2), 279–292. https://doi.org/10.1007/s11064-006-9165-0
30. Bénardais K, Kotsiari A, Škuljec J, Koutsoudaki PN, Gudi V, Singh V, Vulinović F, Skripuletz T, Stangel M (2013) Cuprizone [bis(cyclohexylidenehydrazide)] is selectively toxic for mature oligodendrocytes. Neurotox Res 24(2), 244–250. https://doi.org/10.1007/s12640-013-9380-9
31. Bonetto G, Charalampopoulos I, Gravanis A, Karagogeos D (2017) The novel synthetic microneurotrophin BNN27 protects mature oligodendrocytes against cuprizone-induced death,

through the NGF receptor TrkA. Glia 65(8), 1376–1394. https://doi.org/10.1002/glia.23170

32. Gómez Pinto LI, Rodríguez D, Adamo AM, Mathieu PA (2018) TGF-β pro-oligodendrogenic effects on adult SVZ progenitor cultures and its interaction with the Notch signaling pathway. Glia 66(2), 396–412
33. Hutchins JB (1995) Platelet-derived growth factor receptors of mouse central nervous system cells *in vitro*. J Comp Neurol. 360(1):59-80. doi: 10.1002/cne.903600106
34. Franco PG, Pasquini JM, Silvestroff L (2015) Optimizing culture medium composition to improve oligodendrocyte progenitor cell yields *in vitro* from subventricular zone-derived neural progenitor cell neurospheres. PLoS One 10(4), 1–21 https://doi.org/10.1371/journal.pone.0121774
35. Silvestroff L, Franco PG, Pasquini JM (2012b) ApoTransferrin: Dual Role on Adult Subventricular Zone-Derived Neurospheres. PLoS One 7(3): e33937. doi:10.1371/journal.pone.0033937
36. Silvestrof L, Franco P, Pasquini JM (2013) Neural and oligodendrocyte progenitor cells: transferrin effects on cell proliferation. ASN Neuro 5(1):art:e00107. doi:10.1042/AN20120075
37. Vega-Riquer JM, Mendez-Victoriano G, Morales-Luckie RA, Gonzalez-Perez O (2019) Five Decades of Cuprizone, an Updated Model to Replicate Demyelinating Diseases. Curr Neuropharmacol 17(2). https://doi.org/10.2174/1570159x15666170717120343
38. Matsushima GK, Morell P (2001) The neurotoxicant, cuprizone, as a model to study demyelination and remyelination in the central nervous system. Brain Pathol 11(1), 107–116. https://doi.org/10.1111/j.1750-3639.2001.tb00385.x
39. Zhan J, Mann T, Joost S, Behrangi N, Frank M, Kipp M (2020) The Cuprizone Model: Dos and Do Nots. Cells 9(4), 843. https://doi.org/10.3390/cells9040843
40. Brazel CY, Limke TL, Osborne JK, Miura T, Cai J, Pevny L, Rao MS (2005) Sox2 expression defines a heterogeneous population of neurosphere-forming cells in the adult murine brain. Aging Cell 4(4), 197–207. https://doi.org/10.1111/j.1474-9726.2005.00158.x
41. Zhang J, Jiao J (2015) Molecular Biomarkers for Embryonic and Adult Neural Stem Cell and Neurogenesis. Biomed Res Int 2015 :727542. https://doi.org/10.1155/2015/727542
42. Ellis P, Fagan BM, Magness ST, Hutton S, Taranova O, Hayashi S, McMahon A, Rao M, Pevny L (2004) SOX2, a persistent marker for multipotential neural stem cells derived from embryonic stem cells, the embryo or the adult. Dev Neurosci 26(2–4), 148–165. https://doi.org/10.1159/000082134
43. Gallo V, Götz M (2015) Glial stem and progenitor cells shape the brain-in ontogeny, phylogeny, and disease. Glia 63(8), 1288–1290. https://doi.org/10.1002/glia.22860
44. Merkle FT, Tramontin AD, Garcia-Verdugo JM, Alvarez-Buylla A (2004) Radial glia give rise to adult neural stem cells in the subventricular zone. Proc Natl Acad Sci U S A 101(50), 17528–17532. https://doi.org/10.1073/pnas.0407893101
45. Alves JAJ, Barone P, Engelender S, Fróes MM, Menezes JRL (2002) Initial stages of radial glia astrocytic transformation in the early postnatal anterior subventricular zone. J Neurobiol 52(3), 251–265. https://doi.org/10.1002/neu.10087

46. Guo Z, Wang X, Xiao J, Wang Y, Lu H, Teng J, Wang W (2013) Early postnatal GFAP-expressing cells produce multilineage progeny in cerebrum and astrocytes in cerebellum of adult mice. Brain Res 1532, 14–20. https://doi.org/10.1016/j.brainres.2013.08.003
47. Jensen JB, Parmar M, Strengths and limitations of the neurosphere culture system. Mol Neurobiol 34, 153–161 (2006). https://doi.org/10.1385/MN:34:3:153
48. Reynolds BA, Weiss S (1996) Clonal and Population Analyses Demonstrate That an EGF-Responsive Mammalian Embryonic CNS Precursor Is a Stem Cell. Dev Biol 175(1), 1–13. https://doi.org/10.1006/dbio.1996.0090
49. Soares R, Ribeiro FF, Lourenço DM, Rodrigues RS, Moreira JB, Sebastião AM, Morais VA, Xapelli S (2020) Isolation and Expansion of Neurospheres from Postnatal (P1–3) Mouse Neurogenic Niches. J. Vis. Exp (159), e60822, doi:10.3791/60822
50. Jackson EL, Garcia-Verdugo JM, Gil-Perotin S, Roy M, Quinones-Hinojosa A, VandenBerg S, Alvarez-Buylla A (2006) PDGFR alpha-positive B cells are neural stem cells in the adult SVZ that form glioma-like growths in response to increased PDGF signaling. Neuron 51(2), 187–199. https://doi.org/10.1016/j.neuron.2006.06.012
51. Ishii Y, Matsumoto Y, Watanabe R, Elmi M, Fujimori T, Nissen J, Cao Y, Nabeshima Y, Sasahara M, Funa K (2008) Characterization of neuroprogenitor cells expressing the PDGF beta-receptor within the subventricular zone of postnatal mice. Mol Cell Neurosci 37(3), 507–518. https://doi.org/10.1016/j.mcn.2007.11.006
52. Chojnacki A, Mak G, Weiss S (2011) PDGFRα expression distinguishes GFAP-expressing neural stem cells from PDGF-responsive neural precursors in the adult periventricular area. J Neurosci 31(26), 9503–9512. https://doi.org/10.1523/JNEUROSCI.1531-11.2011
53. Gil-Perotín S, Duran-Moreno M, Cebrián-Silla A, Ramírez M, García-Belda P, García-Verdugo JM (2013) Adult neural stem cells from the subventricular zone: A review of the neurosphere assay. Anat Rec (Hoboken) 296(9), 1435–1452. https://doi.org/10.1002/ar.22746
54. Hillis JM, Davies J, Mundim MV, Al-Dalahmah O, Szele FG (2016) Cuprizone demyelination induces a unique inflammatory response in the subventricular zone. J Neuroinflammation 13(1), 190. https://doi.org/10.1186/s12974-016-0651-2
55. Le Belle JE, Orozco NM, Paucar AA, Saxe JP, Mottahedeh J, Pyle AD, Wu H, Kornblum HI (2011) Proliferative neural stem cells have high endogenous ROS levels that regulate self-renewal and neurogenesis in a PI3K/Akt-dependant manner. Cell Stem Cell 8(1), 59–71. https://doi.org/10.1016/j.stem.2010.11.028
56. Morrell A, Tallino S, Yu L, Burkhead JL (2017) The role of insufficient copper in lipid synthesis and fatty-liver disease. IUBMB Life 69(4), 263–270. https://doi.org/10.1002/iub.1613
57. Madhavan L, Ourednik V, Ourednik J (2006) Increased “Vigilance” of Antioxidant Mechanisms in Neural Stem Cells Potentiates Their Capability to Resist Oxidative Stress. Stem Cells 24(9), 2110–2119. https://doi.org/10.1634/stemcells.2006-0018

58. Romanko MJ, Rothstein RP, Levison SW (2004) Neural stem cells in the subventricular zone are resilient to hypoxia/ischemia whereas progenitors are vulnerable. J Cereb Blood Flow Metab 24(7), 814–825. https://doi.org/10.1097/01.WCB.0000123906.17746.00
59. Limoli CL, Giedzinski E, Baure J, Doctrow SR, Rola R, Fike JR (2006) Using superoxide dismutase/catalase mimetics to manipulate the redox environment of neural precursor cells. Radiat Prot Dosimetry 122(1–4), 228–236. https://doi.org/10.1093/rpd/ncl458
60. Prozorovski T, Schulze-Topphoff U, Glumm R, Baumgart J, Schröter F, Ninnemann O, Siegert E, Bendix I, Brüstle O, Nitsch R, Zipp F, Aktas O (2008) Sirt1 contributes critically to the redox-dependent fate of neural progenitors. Nat Cell Biol 10(4), 385–394. https://doi.org/10.1038/ncb1700
61. Zhou D, Shao L, Spitz DR (2014) Reactive oxygen species in normal and tumor stem cells. Adv Cancer Res 122, 1–67. https://doi.org/10.1016/B978-0-12-420117-0.00001-3
62. Nugud A, Sandeep D, El-Serafi AT (2018) Two faces of the coin: Minireview for dissecting the role of reactive oxygen species in stem cell potency and lineage commitment. J Adv Res 14, 73–79. https://doi.org/10.1016/j.jare.2018.05.012
63. Chiang YH, Silani V, Zhou FC (1996) Morphological differentiation of astroglial progenitor cells from EGF-responsive neurospheres in response to fetal calf serum, basic fibroblast growth factor, and retinol. Cell Transplant 5:179–189. doi:10.1016/0963-6897(95)02043-8
64. Brunet JF, Grollimund L, Chatton JY, Lengacher S, Magistretti PJ, Villemure JG, Pellerin L (2004) Early acquisition of typical metabolic features upon differentiation of mouse neural stem cells into astrocytes. Glia 46:8–17. doi:10.1002/glia.10348

Tables

Table 1
Primary antibodies used for Immunofluorescent detection

Antibody	Cell detection	Host species and clonality	Supplier and catalog #	RRID	Dilution
anti Sox2	NSC/NPC	Rabbit polyclonal	Abcam Ab97959	AB_2341193	1:200
anti Sox10	Oligodendroglial lineage	Rabbit monoclonal	Abcam ab155279	AB_2650603	1:200
anti PDGFRα	OPC-pre OL	Goat polyclonal	Neuromics GT15150	AB_2737233	1:200
anti GFAP	NSC/Astrocytes	Mouse monoclonal Cy3 conjugated	Sigma-Aldrich C9205	AB_476889	1:500 for IHC 1:750 for ICC
anti βTubulin III (Tuj1)	Neuroblasts	Mouse monoclonal	Sigma-Aldrich T8578	AB_1841228	1:200
anti Olig2	Oligodendroglial lineage	Rabbit polyclonal	Millipore AB9610	AB_570666	1:100
anti NG2	OPC/pre-OL	Rabbit polyclonal	Millipore AB5320	AB_11213678	1:200
anti MBP	Mature OL	Mouse monoclonal	Biolegend 808401	AB_2564741	1:750
anti BrdU	Proliferative cell	Mouse monoclonal	Roche B2531	AB_476793	1:100
anti A2B5	Oligodendrocyte-type-2 astrocyte (O-2A) progenitor cells	Mouse monoclonal	Provided by Dr Campagnoni (Mental Retardation Research Center, University of California)	-	1:50
anti-Carbonic Anhydrase II (CAII)	OL lineage	Rabbit polyclonal	Provided by Dr. J Pasquini	-	1:200

List of antibodies used in this study. NSC: Neural stem cells, NPC: Neural progenitor cells, OPC: oligodendroglial precursor cells, pre OL: pre-oligodendrocytes, GFAP: Glial fibrillary acidic protein, OL: oligodendrocyte, BrdU: bromodeoxyuridine, RRID: Research resource identifier, IHC: immunohistochemistry, ICC: Immunocytochemistry.

Figures

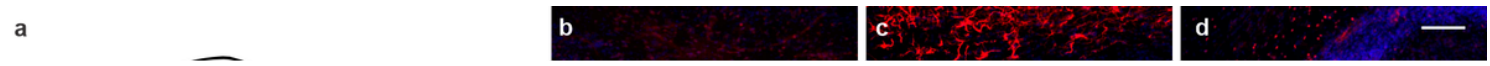

Figure 1

The neonatal brain as a cell source for NS cultures. **a** Schematic representation of a 4-day-old mouse brain adapted from Allen Developing Mouse Brain Atlas, (RRID:SCR_002990, http://developingmouse.brain-map.org/). The red box indicates the area of analysis of brain sections shown in images **b**-**g**. **b**-**g** Immunohistochemical analysis showing the expression patterns of Sox2 (**b**), GFAP (**c**), Olig2 (**d**), Sox2 (**e**), PDGFRα (**f**) and NG2 (**g**) in the selected area shown in **a**. NUC: Höechst stained nuclei are in blue. Scale bar in **d**: 100 μm for images **b**-**g**. CC: corpus callosum, LV: lateral ventricle, CP: caudate putamen, CX: cortex, SVZ: subventricular zone

Figure 2

Experimental design. **a** Schematic view of culture protocols. Periventricular brain tissue was dissected, and cells were dissociated in B27 supplemented DMEM/F12. In the presence of bFGF and EGF, neurospheres (NS) begin to form in suspension after a few days. According to the experiment design, whole NS were attached to poly-L-lysine coated coverslips and maintained in proliferation media for migration analysis. Alternatively, NS were dissociated, and cells were plated to study the cell differentiation process in a growth factor-free medium. **b** Bright field view of NS in suspension, cultured for one week in proliferative conditions. **c** GFAP expression in NS after one day in culture after attachment to a poly-L-lysine coated surface. **d** Representative NS after two days in adhesion, showing GFAP expression upregulation and $GFAP^{+}$ cell processes elongation. **e** Dissociated NS cells in proliferative conditions expressed the NSC/NPC marker Sox2 and incorporated BrdU. For differentiation studies, dissociated NS cells were cultured without growth factors. The expression of several markers for different cell types such as Sox2 (**f**), PDGFRα (**g**) and CAII (**h**) for oligodendroglial lineage; A2B5 (**i**) for glial progenitor, TujI (**f**) for neurons; GFAP (**g**) for astrocytes; and MBP (**h**) for mature oligodendrocytes was determined by immunofluorescence. Scale bar in **b** represents 100 μm, scale bar in **c** indicates 50 μm for **c** and **d**, and scale bar in **i** corresponds to 100 μm for **e** to **i**

Figure 3

GFP expression in ACT::GFP mice-derived cultures serves as a cell viability marker. **a**-**c** Whole NS from ACT::GFP mice were cultured in adhesion for 6 days in proliferating conditions. Constitutive expression of GFP (green) was detected in every cell in the culture. **d**-**f** NS were dissociated, and cells were cultured without mitogens for differentiation. Although most cells continued expressing GFP, we found some GFP negative pyknotic nuclei (**f**, open arrowheads). **g**-**l** Cultures subjected to stress by starvation were stained with propidium iodide (PI) to detect dead cells. Colocalization analysis revealed that GFP was detected in PI negative living cells (arrowheads) and excluded from PI positive dead cells. Nuclei were stained with Höechst (NUC, blue), GFP expression was detected by green fluorescence (green) and dead cells were identified by propidium iodide staining (PI, red). Scale bar in **c** represents 250 µm for **a**-**c**, scale bar in **f** corresponds to 100 µm for **d**-**f** and scale bar in **i** represents 100 µm for **g**-**l**

Figure 4

CPZ treatment reduces NSC/NPC proliferation without affecting cell survival. **a**-**h** Representative images of floating NS cultures grown for 6 days in proliferating media with 0 to 1000 µM CPZ. CTL represents control cultures without any treatment. NS numbers for each CPZ concentration (**i**) and NS diameter (**j**) were registered and analyzed by One way ANOVA and Bonferroni post-test, *p<0.05 compared to CPZ0. **k**-**m** BrdU incorporation assay in dissociated cultures grown in proliferative media from CPZ0 (**k**) and CPZ1000 (**l**) (red). Nuclei were stained with Höechst (blue). The percentage of proliferating cells after 1-hour BrdU pulse was analyzed by Student T test (M), *** p<0.001. Scale bar in **h** represents 100 µm for **a**-**h**. Scale bar in **l** represents 100 µm for **k**-**l**

Figure 5

CPZ treatment enhances cell migration. The effects of CPZ treatments were evaluated on migratory patterns of adhered NS from wild type animals. Representative images showing $GFAP^+$ processes elongation (**a**, **b**) and nuclei of migratory cells (**d**, **e**) after vehicle (CPZ0) (**a**, **d**) or 1000µM CPZ treatments (CPZ1000) (**b**, **e**). **c** Maximal migration distance was determined by measuring the radius of the migratory area (dotted line in **a**, **b**, **d**, **e**). **f** Numbers of nuclei detached from each NS were also evaluated and compared between conditions. Migration distance from the NS edge was determined for every individual nucleus within a quadrant (**g**, **h**) and mean cell migration was calculated for all tested CPZ doses (**i**). Statistical analysis was performed by measuring 10 to 15 NS per coverslip by triplicate and analyzed by

One way ANOVA and Bonferroni post-test in comparison to CPZ0 (**c**, **f**, **i**), *p<0.05, ***p<0.001. Heat map graphs were built to show representative nuclei density distribution around NS treated with CPZ0 (**j**) or CPZ1000 (**k**). Scale bar in **h** represents 250 µm for **a**, **b**, **d**, **e**, **g** and **h**

Figure 6

CPZ treatment promotes reactive oxygen species overproduction in proliferating cultures. **a** Basis of intracellular ROS measurement by using H_2DCFDA probe. After non fluorescent H_2DCFDA is internalized into cells, it is deacetylated by intracellular esterases. The product H_2DCF, which is retained inside the cell, is then oxidized in the presence of ROS, generating the highly fluorescent product DCF. **b**-**c** Representative fluorescent microscopy images showing dissociated NS cells treated with CPZ0 and CPZ1000 for 24 hours in proliferating media and incubated with H_2DCFDA for DCF detection. Scale bar in **c** represents 250 µm for **b**-**c**. **d** Quantification of DCF fluorescence after H_2DCFDA incubation, relativized to Höechst nuclear staining by using a multi-well plate fluorometer in proliferating cultures treated with CPZ at different doses for 24 hours. Statistical analysis was performed by One way ANOVA and Bonferroni post-test, *p<0.05 and ***p<0.001 indicate significance in comparison to CPZ0. **e** Time course of DCF production in CPZ0 and CPZ1000 treated cultures by fluorometric analysis. Statistical analysis was performed by Two-way ANOVA and Bonferroni post-test, *p<0.05. (F-H) Dot plots of flow cytometry data showing side scatter channel (SSC) vs DCF fluorescence intensity after 24 hours of CPZ0 (**f**) and CPZ1000 (**g**) treatments. **h** Hydrogen peroxide-induced oxidative stress (H_2O_2) was used as a positive control. Cell percentages of low, medium, or high DCF fluorescence are indicated in each graph

Figure 7

CPZ decreases general survival of differentiating cultures without affecting neural lineage proportions. **a**-**c** The effect of CPZ treatments on the survival of differentiating cultures was evaluated by determining the percentage of viable GFP expressing cells in ACT::GFP-derived cultures. **c** General cell viability was decreased by CPZ in a dose dependent manner. Statistical analysis was performed by One-way ANOVA and Bonferroni post-test and compared to CPZ0, **p<0.01, ***p<0.001, *ns* non-significant. Immunodetection of MBP (**d**, **g**), Tuj1 (**e**,**h**) and GFAP (**f**, **i**) (red), was relativized to GFP^+ cells (green). Höechst staining of nuclei is in blue. Proportions of MBP^+ oligodendrocytes (**j**), $Tuj1^+$ neurons (**k**) or $GFAP^+$ astrocytes (**l**) were not affected by CPZ treatments. Differences in **j**-**l** were non-significant by One-way ANOVA and Bonferroni post-test. Dot plots of flow cytometry data showing side scatter channel (SSC) vs DCF fluorescence intensity in CPZ0 (**m**) and CPZ1000 (**n**) conditions. Neural lineage proportions from wild type mice-derived cultures were compared between cells grown in serum free (**o**) and FCS

supplemented media (**p**). The total number of nuclei in the CTL was set as the 100% for comparison with all other conditions. Inside each bar, proportions of MBP^+ oligodendrocytes (green), $GFAP^+$ astrocytes (blue) and $TUJI^+$ neurons (red) are indicated. Gray bars correspond to unstained cell for these markers, which were estimated by subtraction of MBP, GFAP and TUJI percentages from nuclei for each condition. For simplicity, error bars were omitted and only the means are shown in the graph. Scale bar in **f** equals 100 µm for **a**-**b** and **d**-**i**.

Figure 8

CPZ affects mature oligodendrocyte survival. Immunocytochemical analysis for MBP was performed in NS-dissociated cells from ACT::GFP transgenic animals cultured for 6 days in proliferating conditions and six additional days in differentiating conditions. Starting experimental point (PRE) corresponds to differentiated cells before CPZ treatments begin (**a**-**c**). Cells were treated with CPZ at several concentrations for two days and analyzed for GFP expression and MBP immunofluorescence (**d**-**m**). The percentage of viable GFP^+ cells (**n**) and mature MBP^+ oligodendrocytes (**o**) were compared between conditions and data were analyzed by One-way ANOVA and Bonferroni post-test. Statistical significance over bars refer to the comparison with CPZ0, while the hashtag over the line is for comparison with PRE-condition, # $p<0.1$, ** $p<0.05$ and *** $p<0.01$. Scale bar in **l** equals 100 µm for **a**, **d**, **f**, **h**, **j** and **l**, scale bar in **m** equals 100 µm for **b**, **e**, **g**, **i**, **k** and **m**. Representative images from adhered NS treated with CPZ0 (**p**) or CPZ500 (**q**) showing MBP^+ cell distribution around the NS. GFP expression is shown in green, MBP immunodetection is in red and nuclei are stained in blue with Höechst. Scale bar in **q** equals 100 µm for **p** and **q**

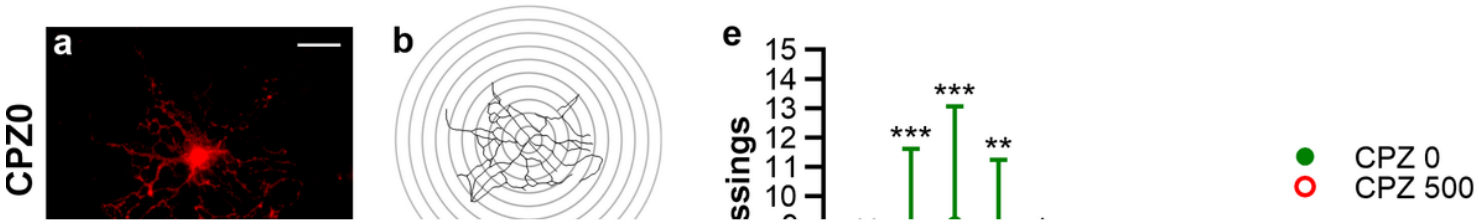

Figure 9

Sholl analysis to determine OL morphological complexity in differentiated NS cultures treated with CPZ. Representative images of MBP^+ OL after treatment with CPZ0 (**a**, **b**) or CPZ500 (**c**, **d**). OL processes were outlined and centered in a 10 μm spaced-ring grid by using the Sholl analysis plugin for ImageJ (**b**, **d**). The mean of processes crossing per ring were analyzed by One-way ANOVA and Bonferroni post-test (**e**). Statistical significance *** $p<0.001$; ** $p<0.01$; * $p<0.05$

Figure 10

CPZ effects on differentiated neural lineages. Quantitation of $GFAP^+$ astrocytes (**a**), $PDGFR\alpha^+$ oligodendroglial precursor cells (**b**) and $Tuj1^+$ neurons (**c**) by immunocytochemistry in ACT::GFP dissociated NS cultures differentiated for six days and then treated with CPZ for 2 days. For each marker, the percentage respect to GFP^+ viable cells is shown. Statistical analysis was performed by One-way ANOVA and Bonferroni multiple comparison post-test (*ns*: non-significant). **d**-**g** Wild type mice-derived intact NS were plated and differentiated in adhesion for 6 days in control media and then treated with CPZ0 or CPZ500 for 2 additional days**.** Immunofluorescence of cells showing PDGFRα and MBP (**d**, **e**), or GFAP and Tuj1 (**f**, **g**) markers. Scale bar in **d** equals 200 μm for **d**-**g**

Figure 11

Models of CPZ effects on neural cells *in vivo*. **a** CPZ effects on mature oligodendrocytes**.** OL loss represents the main feature of demyelinating diseases such as Multiple Sclerosis. CPZ treatment directly or indirectly affects mature oligodendrocytes by inducing OL death both *in vivo* and *in vitro*. In the *in vivo* context, damage to OL occurs in concert with the increment in the numbers of reactive astrocytes and activated microglia. Signals from this pathological scenario led to the activation of both local OPC as well as NSC/NPC pools to start the regenerative process. After activation of NSC proliferation and migration of progenitors, cells are committed to the oligodendroglial lineage that differentiate into mature OL. This basic cellular model could only explain some features of demyelination and remyelination in the acute CPZ model. **b** CPZ effects on NSC/NPC. From our data, we hypothesized additional effects of CPZ on several steps during oligodendrogenesis from NSC/NPC. Concomitant to CPZ damage to mature OL, that activates NSC proliferation, CPZ directly inhibits NSC/NPC proliferation and enhances migration of progenitors, probably by the induction of ROS overproduction. CPZ also reduces the survival of cells undergoing cell differentiation. By these CPZ overlapping mechanisms, on different cell types, it is possible to explain remyelination failure *in vivo* in the chronic CPZ model by the long- term exhaustion of NSC/NPC pools which prevents the generation of new OL